ARTICLE

GRIN2D Recurrent De Novo Dominant Mutation Causes a Severe Epileptic Encephalopathy Treatable with NMDA Receptor Channel Blockers

Dong Li,[1,14] Hongjie Yuan,[2,14] Xilma R. Ortiz-Gonzalez,[3,4,14] Eric D. Marsh,[3,4,14] Lifeng Tian,[1] Elizabeth M. McCormick,[1,5] Gabrielle J. Kosobucki,[6] Wenjuan Chen,[2] Anthony J. Schulien,[6] Rosetta Chiavacci,[1] Anel Tankovic,[2] Claudia Naase,[7] Frieder Brueckner,[8] Celina von Stülpnagel-Steinbeis,[9,10] Chun Hu,[2] Hirofumi Kusumoto,[2] Ulrike B.S. Hedrich,[11] Gina Elsen,[11] Konstanze Hörtnagel,[12] Elias Aizenman,[6] Johannes R. Lemke,[13,15] Hakon Hakonarson,[1,4,5,15] Stephen F. Traynelis,[2,15] and Marni J. Falk[4,5,15,*]

N-methyl-D-aspartate receptors (NMDARs) are ligand-gated cation channels that mediate excitatory synaptic transmission. Genetic mutations in multiple NMDAR subunits cause various childhood epilepsy syndromes. Here, we report a de novo recurrent heterozygous missense mutation—c.1999G>A (p.Val667Ile)—in a NMDAR gene previously unrecognized to harbor disease-causing mutations, *GRIN2D,* identified by exome and candidate panel sequencing in two unrelated children with epileptic encephalopathy. The resulting GluN2D p.Val667Ile exchange occurs in the M3 transmembrane domain involved in channel gating. This gain-of-function mutation increases glutamate and glycine potency by 2-fold, increases channel open probability by 6-fold, and reduces receptor sensitivity to endogenous negative modulators such as extracellular protons. Moreover, this mutation prolongs the deactivation time course after glutamate removal, which controls the synaptic time course. Transfection of cultured neurons with human *GRIN2D* cDNA harboring c.1999G>A leads to dendritic swelling and neuronal cell death, suggestive of excitotoxicity mediated by NMDAR over-activation. Because both individuals' seizures had proven refractory to conventional anti-epileptic medications, the sensitivity of mutant NMDARs to FDA-approved NMDAR antagonists was evaluated. Based on these results, oral memantine was administered to both children, with resulting mild to moderate improvement in seizure burden and development. The older proband subsequently developed refractory status epilepticus, with dramatic electroclinical improvement upon treatment with ketamine and magnesium. Overall, these results suggest that NMDAR antagonists can be useful as adjuvant epilepsy therapy in individuals with *GRIN2D* gain-of-function mutations. This work further demonstrates the value of functionally evaluating a mutation, enabling mechanistic understanding and therapeutic modeling to realize precision medicine for epilepsy.

Introduction

The epileptic encephalopathies, a spectrum of conditions manifesting with intractable seizures and neurodevelopmental disabilities, have a diverse range of etiologies including an increasing number of monogenic disorders. Establishing the precise genetic etiology in individuals has become increasingly possible in the rapidly advancing age of massively parallel sequencing analyses. However, pursuit of clinically available molecular studies is able to provide a definitive diagnosis only in an estimated 25% to 41% of such cohorts.[1–4] The likelihood of success is increased if broad-based exome- or genome-sequencing studies are pursued in familial trios, because this allows the ready detection of biparentally inherited mutations, as well as detection of de novo dominant mutations. De novo variants are increasingly appreciated to be a common genetic basis for the epileptic encephalopathies and neurodevelopmental disorders.[5] Still, the clinical laboratory diagnosis of pathogenic mutations is limited to prior-defined genes. Identification of either variants of uncertain significance in prior-defined genes or predicted pathogenic mutations in genes previously unrecognized to have disease-causing mutations poses challenges for clinical diagnosis. In either scenario, confidence in establishing the correct disease etiology can be garnered by identifying multiple individuals having similar variants in the same gene who share similar

[1]Center for Applied Genomics, Department of Pediatrics, The Children's Hospital of Philadelphia, Philadelphia, PA 19104, USA; [2]Department of Pharmacology and Center for Functional Evaluation of Rare Variant (CFERV), Emory University School of Medicine, Rollins Research Center, Atlanta, GA 30322, USA; [3]Division of Neurology, The Children's Hospital of Philadelphia, Philadelphia, PA 19104, USA; [4]University of Pennsylvania Perelman School of Medicine, Philadelphia, PA 19104, USA; [5]Division of Human Genetics, Department of Pediatrics, The Children's Hospital of Philadelphia, Philadelphia, PA 19104, USA; [6]Department of Neurobiology, Pittsburgh Institute for Neurodegenerative Diseases, University of Pittsburgh School of Medicine, Pittsburgh, PA 15261, USA; [7]Children's Hospital Bayreuth, 95445 Bayreuth, Germany; [8]Institute for Neuropediatrics and Social Pediatrics Hamburg East, 22111 Hamburg, Germany; [9]Hospital for Neuropediatrics and Neurological Rehabilitation, Epilepsy Center for Children and Adolescents, 83569 Vogtareuth, Germany; [10]Institute for Transition, Rehabilitation and Palliation in Children and Adolescents, Paracelsus Medical University Salzburg, 5020 Salzburg, Austria; [11]Department of Neurology and Epileptology, Hertie Institute for Clinical Brain Research, University of Tübingen, 72076 Tübingen, Germany; [12]CeGaT GmbH, 72076 Tübingen, Germany; [13]Institute of Human Genetics, University of Leipzig Hospitals and Clinics, 04103 Leipzig, Germany
[14]These authors contributed equally to this work
[15]These authors contributed equally to this work
*Correspondence: falkm@email.chop.edu
http://dx.doi.org/10.1016/j.ajhg.2016.07.013.

phenotypic presentations. However, reaching definitive confirmation of the disease etiology, as well as mechanistic insight into the disease process, requires functional validation in cellular and/or animal model systems. Indeed, such insights become critical to develop and test targeted therapies that are tailored to the specific underlying pathophysiology of rare Mendelian disorders.

N-methyl-D-aspartate receptors (NMDARs) are ligand-gated cation channels that mediate a slow calcium-permeable component of excitatory synaptic transmission in brain.[6] NMDAR mutations (*GRIN1* [MIM: 138249], *GRIN2A* [MIM: 138253], *GRIN2B* [MIM: 138252]) have been identified in neurological disorders, including epilepsy.[7–11] Here, we report a genetic disorder caused by a de novo, recurrent, missense mutation c.1999G>A (p.Val667Ile) in *GRIN2D* (MIM: 602717) that was identified by exome and panel sequencing in two unrelated children with epileptic encephalopathy. Two affected individuals were recruited under research protocols approved by their respective institutions' IRB with informed consent. The family of each subject sequenced provided written consent and all work was in accordance with proper IRB-approved protocol. Extensive functional characterization of this NMDAR mutation in heterologous expression systems revealed that its pathogenicity is multifactorial. Indeed, it was found to reflect a combination of enhanced charge transfer during channel activation derived from its reduced sensitivity to negative allosteric modulators, prolongation of the synaptic response time course, increased probability that agonist-bound receptors will open, and increased response to submaximal concentrations of agonists.

Because seizures in both affected children were refractory to conventional antiepileptic medications, in vitro pharmacologic studies were performed to test the sensitivity of mutant receptors to FDA-approved NMDAR antagonists. Based on these data, oral memantine was used off-label as adjunctive therapy in both children and led to a modest improvement in seizure control in one of them and parental reports of developmental improvements in both. The older proband was taken off memantine and months later her seizures became near continuous, at which point she was treated for subclinical status epilepticus. Although her subclinical status was refractory to both midazolam- and pentobarbital-induced coma, a uniquely synergistic therapy of ketamine and magnesium was tried based on the in vitro data that remarkably led to seizure freedom and dramatic electroencephalogram (EEG) as well as clinical improvement. These results suggest that NMDAR antagonists and magnesium might be useful adjunctive therapy to control seizures in individuals with *GRIN2D* gain-of-function mutations in pore-forming regions of the receptor. This further demonstrates the promise of personalizing therapeutic regimens to functionally validated genetic etiologies and specific disease mechanisms.

Material and Methods

Molecular Studies

Whole-Exome Sequencing and Bioinformatics Analytic Methods Performed in Proband 1

After institutional review board (IRB)-approved informed consent, blood was obtained from proband 1 and ultimately both of her unaffected parents. Exome sequencing was performed only on the proband and her mother, however, because her father was not available at the beginning of the study. Exons were captured from qualified fragmented genomic DNA samples using the SureSelect Human All Exon 51 Mb kit (Agilent Technologies). Paired-end 101-base massively parallel sequencing was carried out on the Illumina HiSeq2000 platform (Illumina), according to the manufacture's protocols. Base calling was performed by the Illumina CASAVA software (v.1.8.2) with default parameters. Sequencing reads passing the quality filter were aligned to the human reference genome (GRCh37-derived alignment set used in 1000 Genomes Project) with Burrows-Wheeler aligner (BWA v.0.6.2).[12] PCR duplicates were removed with Picard (v.1.97). The Genome Analysis Toolkit (GATK v.2.6)[13] was used to recalibrate base quality scores, realign around insertions/deletions (indels), and generate variant calls. All variants were then annotated by ANNOVAR[14] and SnpEff (v.2.0.5)[15] to collect amino acid change, protein functional effect, conservation score, minor allele frequency (MAF), and output from prediction programs (SIFT, PolyPhen-2, LRT, and MutationTaster). Variants were prioritized under both autosomal-dominant and -recessive models to exclude variants with the following factors: (1) synonymous variants, (2) variants in known pseudogenes, (3) variants having a MAF of greater than or equal to 1% in either the 1000 Genomes Project or the 6,503 exomes from the National Heart, Lung, and Blood Institute Exome Sequencing Project (ESP6500SI), (4) variants having a conservation score GERP++ less than 2, and (5) variants that were predicted by SIFT/PolyPhen-2 scores to be benign. After filtering, no potentially candidate with paired mutations in a gene survived. To facilitate identification of de novo dominant variants, we presumed that the variants responsible for the disease would be rare and probably absent in the general population. Therefore, we selected for variants not present in 1000 Genomes Project and not identified in control subjects by our in-house exome variant database. The de novo dominant variants identified were then further filtered to exclude variants that had a MAF of greater than 0.05% in ESP6500SI. Validation of surviving dominant mutation candidates was performed by standard Sanger sequencing.

Candidate Gene Panel Sequencing and Bioinformatics Analytic Methods Performed in Proband 2

Genetic testing was performed with a epilepsy panel that includs a few previously unrecognized gene candidates that were largely chosen due to their gene families. Methods were performed as previously described.[16] In brief, coding regions and exon-intron boundaries were enriched using Agilent SureSelect technology followed by next-generation sequencing on the Illumina HiSeq2500 platform. Reads were aligned using Burrows Wheeler Aligner (BWA-mem 0.7.2) with hg19 as reference genome. Unambiguous reads were removed with Picard 1.14. Variant calling was performed with SAMtools (v.0.1.18) and VarScan (v.2.3). Variants

were then selected with a MAF below 5% (according to 1000 Genomes, dbSNP, ESP6500SI, and in-house database). More than 98% of targets had at least 30× coverage. Validation of detected variants and segregation analysis were performed by Sanger sequencing.

Electrophysiology and GluN2D-p.Val667Ile Functional Evaluation

For this study we utilized cDNA for wild-type (WT) human NMDAR GluN1-1a (hereafter GluN1) and GluN2D subunits in pCI-neo (GluN2D; GenBank: NP_015566 and NP_000827.1).[17] The mutant GluN2D was generated by site-directed mutagenesis using the QuikChange protocol (Stratagene). Synthesis and injection of cRNA into *Xenopus laevis* oocytes (obtained from Ecocyte) as well as two-electrode voltage-clamp (TEVC) recordings from oocytes were performed as previously described.[18] The recording solution contained (in mM) 90 NaCl, 1 KCl, 10 HEPES, 0.5 $BaCl_2$, 0.01 EDTA (pH 7.4). The membrane potential was held at −40 mV for all TEVC recordings from oocytes unless otherwise stated. The concentration-response curves were fitted with

$$\text{Response} = 100\% \Big/ \left(1 + (EC_{50} / [\text{agonist}])^{N}\right) \quad \text{(Equation 1)}$$

$$\text{Response}\,(\%) = (100 - \text{minimum}) \Big/ \left(1 - ([\text{concentration}]/IC_{50})^{N}\right) + \text{minimum} \quad \text{(Equation 2)}$$

where N is the Hill slope, EC_{50} is the concentration of the agonist that produces a half-maximal effect, IC_{50} is the concentration of the antagonist that produces a half-maximal effect, and *minimum* is the degree of residual inhibition at a saturating concentration of the antagonist. The channel open probability (P_{OPEN}) can be estimated with the following equation:[19]

$$P_{OPEN} = (\gamma_{MTSEA}/\gamma_{CONTROL}) \times (1/\text{ Potentiation}) \quad \text{(Equation 3)}$$

where γ_{MTSEA} and $\gamma_{CONTROL}$ were estimated from GluN1/GluN2A receptors.[20]

The response time course was evaluated using whole-cell voltage-clamp recordings on transiently transfected HEK293 cells at −60 mV (23°C) with an Axopatch 200B amplifier (Molecular Devices). Recording electrodes (3–5 MΩ) were made from thin wall glass micropipettes (TW150F-4, World Precision Instruments) pulled using a vertical puller (Narishige P-10) and filled with (in mM) 110 D-gluconate, 110 CsOH, 30 CsCl, 5 HEPES, 4 NaCl, 0.5 $CaCl_2$, 2 $MgCl_2$, 5 BAPTA, 2 NaATP, and 0.3 NaGTP (pH 7.35). The external solution contained (in mM) 150 NaCl, 10 HEPES, 30 D-mannitol, 3 KCl, 1.0 $CaCl_2$, 0.01 EDTA at 23°C and pH 7.4. Rapid solution exchange and data analysis were performed as previously described.[19] Deactivation time course after rapid removal of glutamate was fitted with

$$\text{Response} = \text{Amp}_{FAST}\,(\exp(-\text{time} / \text{tau}_{FAST})) + \text{Amp}_{SLOW}\,(\exp(-\text{time} / \text{tau}_{SLOW})) \quad \text{(Equation 4)}$$

Unitary currents from single channels were recorded in excised outside-out patches from transfected HEK293 cells that were exposed to 1 mM glutamate and 50 μM glycine and in an external solution at pH 8.0. Single-channel properties including unitary current, mean channel open time, and open probability within a burst were evaluated in recordings at a holding potential of −80 mV. Recording electrodes were made from thick-wall glass pipettes (G150F-4, Warner Instruments) pulled using a vertical puller (Narishige PP-830), coated with Sylgard (Dow Corning), and then fire-polished to 7.5–11 MΩ. The composition of recording solution and internal solution were the same as used for whole-cell voltage-clamp recording. The data were analyzed using QUB and the mean open time distributions were fitted using ChanneLab (Synaptosoft).

Neuronal Excitotoxicity

All procedures involving the use of animals were reviewed and approved by the University of Pittsburgh IACUC. Mixed neuronal/glial cortical cultures were derived from E17 Sprague Dawley rats and maintained as previously described.[21] Neurons were transfected at 19–20 DIV utilizing Lipofectamine 2000.[22] Cells were transfected with the following plasmid mixtures (total of 2.5 μg total DNA/mL): 0.625 μg pUHC13-3 luciferase, 0.875 μg pEGFP-N1, and 1 μg of either pCIneo (vector), human GluN2D, or human GluN2D-p.Val667Ile. Transfection efficiency was approximately 6%–10%. Half of the transfected cultures were treated with 50 μM memantine until analysis. For morphological examination, cells were visualized 24 hr after transfection at 20× and 60× magnification with a Nikon A1+ confocal microscope. For cell toxicity assays, a luciferase viability assay was employed 48 hr after transfection, as previously described.[23] This assay measures viability only in the transfected cells by determining the expression of luciferase using a commercially available kit (Steadylite, Perkin Elmer). We have previously established that luciferase activity correlates precisely with number of live neurons, as measured with alternative methods.[23] Nonetheless, luciferase toxicity assay results were confirmed by cell counts for selected groups performed by a person blinded to the treatment groups. Counts were performed of GFP-positive cells transfected with either GluN2D or GluN2D-p.Val667Ile. Similar to the luciferase assay, a subset of cells transfected with the mutant subunit were exposed to memantine after the transfection. Counts were performed 72 hr after the initiation of the transfection, in order to ensure that dead cells had disintegrated. Each group consisted of three coverslips, with 30 fields at 20× magnification counted for each coverslip in four independent experiments.

Screening of FDA-Approved NMDAR Antagonists

FDA-approved drugs that act as NMDAR open channel blockers were evaluated using voltage clamp recordings from *Xenopus* oocytes co-expressing GluN1 with the WT or mutant GluN2D. The composite concentration-effect curves were recorded at a holding potential of −40 mV and fitted with the Equation 2 to determine the IC_{50} value.

Statistical Analysis

Data are presented as the mean ± the standard error of the mean, and significance tested using a two-tailed unpaired t test or ANOVA, as appropriate. Significance was set at $p < 0.05$. Analysis of neurotoxicity was performed in a blinded fashion.

Results

Clinical Phenotype

Proband 1

Proband 1 is an 8.5-year-old biracial girl of African American and European descent who presented to Genetics Clinic at The Children's Hospital of Philadelphia for

evaluation since infancy of intractable epilepsy, global developmental delay, and static encephalopathy. After decreased fetal movements noted late in pregnancy, she was born at full-term to a $G_3P_{2\rightarrow3}$ mother with meconium aspiration, stridor, and reflux. Clinical concern for seizures was first noted at 4 months of age due to episodic whole-body tremors as well as daily episodes of eye fluttering with arrest of activity. At the age of 10 months, video EEG monitoring revealed frequent spikes and waves in the posterior quadrants while awake. During sleep, her EEG became hypsarrhythmic with a highly disorganized, high-voltage, and multifocal spike and wave discharge recorded throughout. Proband 1's development, movement disorder, pedigree, extensive diagnostic evaluation, and prior treatment are described in the Supplemental Note. Clinical testing results were unrevealing, leading to performance of research-based whole-exome sequencing analysis, as detailed in Material and Methods.

Proband 2

Proband 2 is a Tunisian girl born at 38 weeks' gestation to a $G_2P_{1\rightarrow2}$ mother after an unremarkable pregnancy; she had congenital hypotonia noted in the neonatal period. Clinical concern for seizures was first raised at 2 months of age due to a several-second episode of right cheek twitching, drooling, tongue deviation, and apnea. At 6 months of age, she experienced two episodes on consecutive days of abnormal tongue movements and cyanosis. EEG revealed sharp and spike wave discharges at the right temporal area. Over the next several weeks, three additional episodes of abnormal tongue movements and a generalized seizure occurred. Her epilepsy proved therapy resistant to standard antiepileptic drugs (phenobarbital, valproic acid, levetiracetam), steroids, and vitamin B6, as her EEGs continued to reveal multifocal spike discharges especially in the bioccipital area. Brain MRI, head ultrasound, and electromyogram (EMG) were normal. Clinical genetic diagnostic testing was limited to a blood karyotype, which was normal. Her developmental history, review of systems, pedigree, results of metabolic testing, and physical examination findings are described in the Supplemental Note. Epilepsy candidate gene panel sequencing was performed on a research basis, as detailed in Material and Methods.

Identification of a Recurrent, De Novo, Heterozygous Mutation in *GRIN2D*

After the whole-exome sequencing data filtering strategy (as described in Material and Methods and Table S1), only seven dominant candidates were present in proband 1 and not in her unaffected mother (Table S2, father's sample was not available at the time of exome analysis; see Supplemental Note for full clinical details). Among these, a missense variant, c.1999G>A (p.Val667Ile), identified in *GRIN2D* (GenBank: NM_000836.2), was selected as the most likely disease-causing candidate based on NMDAR being known to control synaptic plasticity and memory function,[24] and the GluN2D subunit being highly expressed in neonatal brain.[25] This heterozygous mutation was absent from 1000 Genomes Project, ESP6500SI, ExAC v.0.3, or additional exome-sequence data from more than 2,000 samples that we had previously sequenced in our in-house database.[26,27] Sanger sequencing in blood from proband 1 and both parents confirmed that this mutation was present only in proband 1 (Figure 1A). Independently, candidate epilepsy panel sequencing in proband 2 also revealed a c.1999G>A (p.Val667Ile) variant in *GRIN2D* and Sanger sequencing confirmed that the variant occurred de novo (see Material and Methods and Supplemental Note for full clinical details).

The Val667 residue is highly conserved across vertebrate species (Figure 1B), as well as within the four GluN2 subunits, suggesting that it may serve an essential role in NMDAR function. Val667 resides in the M3 transmembrane domain, which forms the membrane-spanning ion channel core, and is located very close to the highly conserved motif (SYTANLAAF) that controls channel gating (Figures 1B and 1C).[20,28,29] The M3 transmembrane helix forms a helical bundle crossing that occludes ion permeation through the central pore, which is considered to be a key component of the channel gate. We hypothesized that replacement of valine by isoleucine at this position leads to a gain of function by either stabilizing the open state of the ion channel pore or lowering the activation energy for channel opening.

Functional Evaluation of the Mutant GluN2D Receptor

The mutant GluN2D-p.Val667Ile was co-expressed with GluN1 in *Xenopus laevis* oocytes and its pharmacological properties were evaluated by two-electrode voltage clamp recording. Agonist potencies (EC_{50}, the agonist concentrations that can produce a half-maximal current response) were determined for glutamate and glycine. NMDARs that contain GluN2D-p.Val667Ile showed a statistically significant 1.5-fold reduction in the EC_{50} value (i.e., increased potency) for glutamate (0.26 μM versus 0.40 μM of wild-type [WT] in the presence of 100 μM glycine) and a 1.7-fold reduction for glycine (0.07 μM versus 0.12 μM of WT in the presence of 100 μM glutamate) (Figures 2A and 2B; Table 1). These data indicated that the observed mutation in the epilepsy probands' NMDAR can be activated by lower concentrations of these co-agonists than those required in wild-type NMDARs.

Proton sensitivity was assessed by comparing the current amplitude at pH 6.8 to that observed at pH 7.6. The data showed that the mutant receptor has more current remaining at pH 6.8 (63% versus 33% in the WT, $p < 0.05$, unpaired t test; Figure 2C; Table 1), suggesting that the mutation produces a substantial reduction in tonic in proton inhibition, which should increase the current flowing through NMDARs when bound by agonist. Together, these data support the idea that GluN2D-p.Val667Ile-containing NMDARs will be overactive as a result of both the increased activation at low concentrations of agonists and the reduced proton inhibition. The resulting enhanced excitatory drive may contribute to the individual's epileptic phenotype.

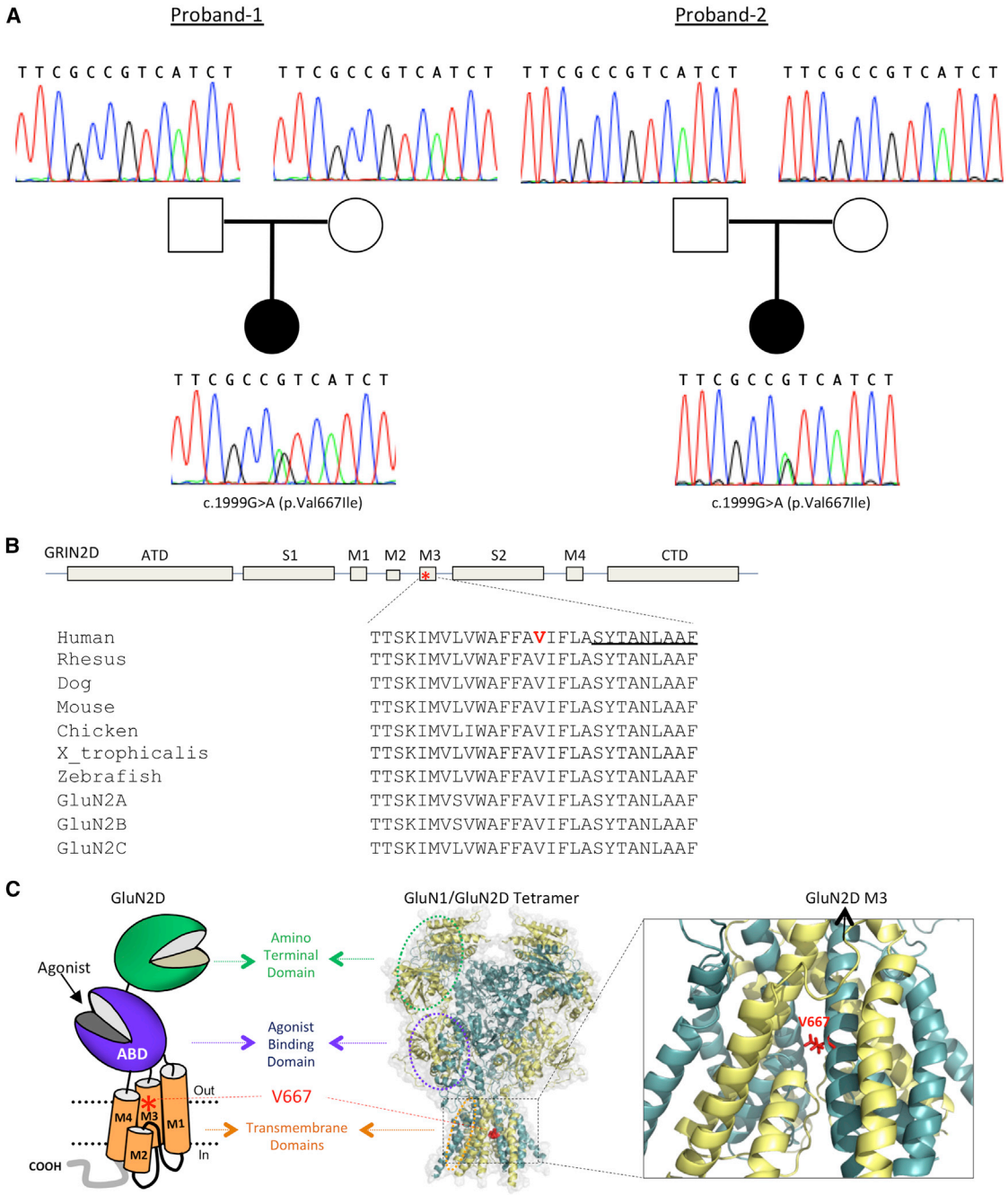

Figure 1. Genetic and Protein Alteration of *GRIN2D* and GluN2D
(A) Pedigrees and genotypes of a de novo mutation c.1999G>A (p.Val667Ile) identified in both unrelated kindreds.
(B) Schematic topology represents a GluN2D subunit, where asterisk indicates the position of the p.Val667Ile variant. The Val667 residue is highly conserved across vertebrate species and all GluN2 subunits.
(C) The red asterisk in the cartoon indicating the domain arrangement of a GluN2D subunit shows the position of Val667 in the transmembrane domain (M3) (left). A homology model of GluN2D subunit, shown as space fill, was built from the GluN1/GluN2B crystallographic data[29,44] using Muscle for sequence alignment, Modeler to build the homology model, and the Schrödinger Modeling for model refinement (middle). The location on the M3 transmembrane helix is show in an expanded panel (right).

Evaluation of Response Time Course and Channel Open Probability of the Mutant GluN2D Receptor

The deactivation time course for NMDAR responses after rapid removal of glutamate controls the time course of the NMDAR component of the excitatory postsynaptic current. We therefore evaluated the effect of GluN2D-p.Val667Ile on the time course of NMDARs in response to rapid application and removal of glutamate (in the presence of saturating glycine). The NMDAR current response time course after glutamate removal was recorded using a piezoelectric rapid solution exchange system and whole-cell patch-clamp recordings of WT

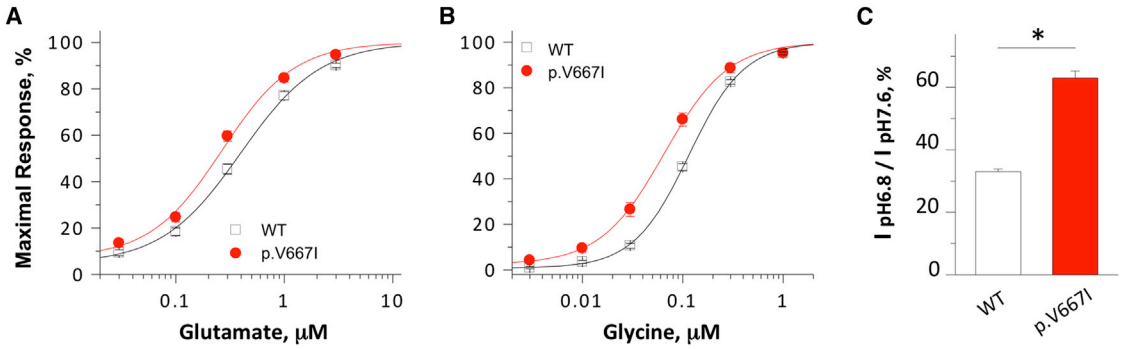

Figure 2. The Mutant GluN2D-p.Val667Ile Changes NMDAR Pharmacological Properties
(A and B) The composite glutamate (in the presence of 100 μM glycine) (A) and glycine (in the presence of 100 μM glutamate) (B) concentration-response curves show an increased agonist potency in the mutant receptors compared to the WT receptors.
(C) Summary of proton sensitivity of WT GluN2D and mutant receptors, evaluated by current ratio at pH 6.8 to pH 7.6. *$p < 0.05$ compared to WT GluN2D, unpaired t test. Error bars show SEM, which were calculated from 20 and 28 independent recordings for WT and mutant receptors, respectively.

GluN1/GluN2D or mutant GluN1/GluN2D-p.Val667Ile co-transfected into HEK293 cells. Although HEK293 cells do not express NMDARs, they have been used extensively to investigate properties of recombinant NMDARs, which show remarkable similarity to properties of native NMDARs.[6] The deactivation time course of the mutant NMDAR after removal of glutamate could be described by two exponential components, which were prolonged in mutant receptors. The weighted time constant (τ_W) from these exponential fits increased from 4,530 ms for the WT NMDARs to 7,020 ms for mutant NMDAR (n = 6; Figures 3A and 3B; Table 2). We also briefly moved the cell into glutamate solution for 5 ms (brief application) to mimic synaptic release of glutamate in the central nervous system. Analysis of the response time course for this paradigm showed that the mutant NMDARs again deactivated with a slower time course (τ_W 6,100 ms) compared to WT GluN1/GluN2D receptors (4,090 ms; Figures 3A and 3B). The slower deactivation time constant is consistent with the increased glutamate potency.[30]

Previous studies have shown that MTSEA (2-aminoethyl methanethiosulfonate hydrobromide) modification of a variant (p.Ala652Cys) within GluN1 SYTANLAAF gating region can lock NMDARs in open state.[20,28] If we assume open probability of the covalently modified receptor increases to a value near 1, the degree of potentiation of the open probability will be reciprocally related to the channel open probability before MTSEA treatment. We used this approach to assess the effects of GluN2D-p.Val667Ile on the channel open probability (see Equation 3 in Material and Methods).[19] The data indicate that agonist-bound mutant channels expressed in oocytes have a 10-fold higher open probability (0.06) than WT receptors (0.006) (Figures 3C and 3D; Table 1).

To further assess the effects of this mutation on NMDAR function, we recorded single-channel currents activated by maximally effective concentration of glutmate and glycine in outside-out patches excised from HEK cells transiently expressing human GluN2/GluN2D receptors. Analysis for WT GluN1/GluN2D receptors gave unitary currents with two prominent sublevels with a chord conductance of 65 ± 1.2 pS and 42 ± 1.2 pS (n = 3) (assuming a reversal potential of 0). Mutant GluN1/GluN2D-p.Val667Ile receptors had similar chord conductance values (67 ± 0.8 pS and 42 ± 0.6 pS, n = 4; p = 0.134 and 0.918, unpaired t test), suggesting that this mutation did not alter the ion permeation properties. However, the mean channel open time increased 6-fold to 5.2 ± 0.03 ms (n = 4) for the mutant compared to 0.76 ± 0.03 ms (n = 3) ($p < 0.01$, unpaired t test) for the WT receptors (Figures 3E and 3F; Table 1). Open probability during stretches of the recording with no double openings also increased 6-fold to 0.48 ± 0.002 (n = 4) from 0.08 ± 0.001 (n = 3; $p < 0.01$, unpaired t test) in WT GluN1/GluN2D receptors. Because outside-out patches in this experiment probably contained more than a single active channel, our measurement of open probability for WT GluN1/GluN2D is an overestimate of the probability that a single channel will open. However, for mutant GluN1/GluN2D-p.Val667Ile receptors, we analyzed only stretches of the data record that contained a single active channel, which were unambiguous given the high open probability. These data further support the classification of this variant as producing a strong gain-of-function, are consistent with the apparent increase in agonist potency (Table 1), and raise the possibility that activation of NMDARs that contain the mutant subunit will enhance neuronal excitability in neurons expressing GluN2D.

Neuronal Excitotoxicity Induced by the Mutant GluN2D Receptor

Over-activation of NMDARs is well known to trigger excitotoxic cell death through excessive influx of calcium (Ca^{2+}).[31] In order to assess the potential toxicity of GluN2D-p.Val667Ile expression, rat cortical neurons were maintained in culture for >20 days and transfected with either WT or mutant NMDAR GluN2D subunits. Neuronal health was assessed both visually at 24 hr and via decrease

Table 1. Summary of Pharmacological and Biophysical Properties

	WT	p.Val667Ile
Glutamate, EC_{50}, μM (n)	0.40 ± 0.04 (42)	0.26 ± 0.02 (43)*
Glycine, EC_{50}, μM (n)	0.12 ± 0.005 (23)	0.07 ± 0.008 (26)*
Proton inhibition, % (n)[a]	33% ± 0.9% (20)	63% ± 2.2% (28)*
Amplitude (peak, pA/pF)	21 ± 8.5	37 ± 6.9*
Amplitude (SS, pA/pF)	19 ± 7.2	35 ± 6.8*
I_{SS}/I_{PEAK}	0.95 ± 0.02	0.95 ± 0.01
Rise time (ms)	8.7 ± 0.3	8.7 ± 0.2
τ_{FAST} (ms)	1,448 ± 154	2,920 ± 490
τ_{SLOW} (ms)	5,735 ± 177	12,377 ± 3,878
$\%\tau_{FAST}$	28%	42%
τ_W (ms)	4,523 ± 84	7,021 ± 565*
Charge transfer, pA × ms/pF	94,233	267,778*
n	6	6
% Potentiation by MTSEA	16,120 ± 2,248	1,412 ± 153
Calculated P_{OPEN}	0.006 ± 0.001	0.06 ± 0.008*
n	22	32
Mean open time, ms	0.76 ± 0.03	5.2 ± 1.2*
n	3	4

*$p < 0.05$, unpaired t test, compared with the wild-type (WT). The EC_{50} for glutamate was determined in 100 μM glycine and the EC_{50} for glycine was determined in 100 μM glutamate. The weighted time constant was calculated by Equation 4. Charge transfer was estimated for the response to 5 ms application of glutamate as the product of amplitude and weighted τ.
[a]The proton sensitivity was assessed by comparing the percent of the current at pH 6.8 to that at pH 7.6.

in luciferase expression as an index of cell viability 48 hr later.[23] Expression of WT GluN2D was relatively innocuous to the cells, with no observable changes in morphology and no significant effect on viability (Figure 4). In contrast, neurons expressing GluN2D-p.Val667Ile showed pronounced dendritic swelling 24 hr after transfection in all experiments. Assessment of the overall viability in these cultures showed that the expression of the mutant GluN2D-p.Val667Ile produced >50% lethality when luciferase was assayed 48 hr after the initiation of transfection. Both the morphological abnormalities and the toxicity in GluN2D-p.Val667Ile-expressing cells could be prevented by the continuous presence of an NMDAR channel blocker, memantine (50 μM) (Figure 4), suggesting that over-activation of the mutant receptor was responsible for its deleterious actions on neurons. Consistent with the results from the luciferase assay, transfection of a construct encoding GluN2D-p.Val667Ile induced cell death assessed by counting viable GFP-expressing cells at 72 hr after transfection, and the neurotoxicity was blocked by memantine (see Figure 4B, insert).

Screening of FDA-Approved NMDAR Antagonists

Because conventional antiepileptic drugs did not provide adequate control of the two probands' seizures, we evaluated several FDA-approved NMDAR antagonists for their ability to inhibit receptors containing GluN2D-p.Val667Ile (Table 2). Of these agents, memantine had been indicated to have anticonvulsant effects in animal models of epilepsy[32] and also has been used previously in children without side effects.[33,34] Interestingly, memantine was previously used to treat one individual with a gain-of-function *GRIN2A* mutation (c.2434C>A [p.Leu812Met]), which was associated with increased sensitivity to agonists, increased open probability, and reduced Mg^{2+} sensitivity.[35] Memantine treatment of that individual with drug-resistant epileptic encephalopathy resulted in a substantial reduction in his seizure burden.[36] In vitro analysis in oocytes indicated that memantine inhibited GluN2D-p.Val667Ile-containing NMDARs with an IC_{50} of 4.0 μM compared with 0.57 μM for the WT GluN2D-containing NMDARs (Figure 5A; Table 2). We also evaluated the inhibition of other FDA-approved NMDAR channel blockers—dextromethorphan, dextrorphan, amantadine, and ketamine—on currents arising from GluN2D-p.Val667Ile-containing NMDARs. Both dextromethorphan and its metabolite dextrorphan showed reduced potency on p.Val667Ile-containing NMDARs in comparison to WT NMDARs (3.3-fold and 4.2-fold, respectively; Table 2). Ketamine, an anesthetic, inhibited the GluN1/GluN2D-p.Val667Ile with an IC_{50} of 8.1 μM compared with 2.2 μM for the WT GluN1/GluN2D (Figure 5B; Table 2). These data indicated that NMDAR channel blockers can reduce GluN2D-p.Val667Ile-mediated NMDAR hyperactivity, although at a modestly reduced potency compared to WT receptors.

Voltage-dependent Mg^{2+} inhibition is an important feature of NMDAR function. The Mg^{2+} inhibition on GluN2D-p.Val667Ile was evaluated by two experiments. The concentration-response curves for Mg^{2+} block showed a small but statistically significant 1.3-fold reduction in potency that was manifest as an increase in the IC_{50} value from 220 μM for WT NMDARs to 346 μM for NMDARs containing GluN2D-p.Val667Ile (−60 mV holding potential; $p < 0.05$, unpaired t test) (Figure 5C; Table 2). Evaluation of the current-voltage relationship (Figure 5D) indicated a comparable current flow in the mutant receptors compared to the WT receptors at negative holding potentials in the presence of 0.3 mM, 1.0 mM, and 3.0 mM of Mg^{2+} (e.g., the current ratio was 0.31 ± 0.03 of p.Val667Ile versus 0.29 ± 0.01 of WT at −45 mV in the presence of 1.0 mM Mg^{2+}, $p = 0.66$, unpaired t test).

Clinical Response of *GRIN2D* Probands to NMDA Receptor Antagonists

After the *GRIN2D* variant was identified and in vitro data were obtained, proband 1 (see Supplemental Note for

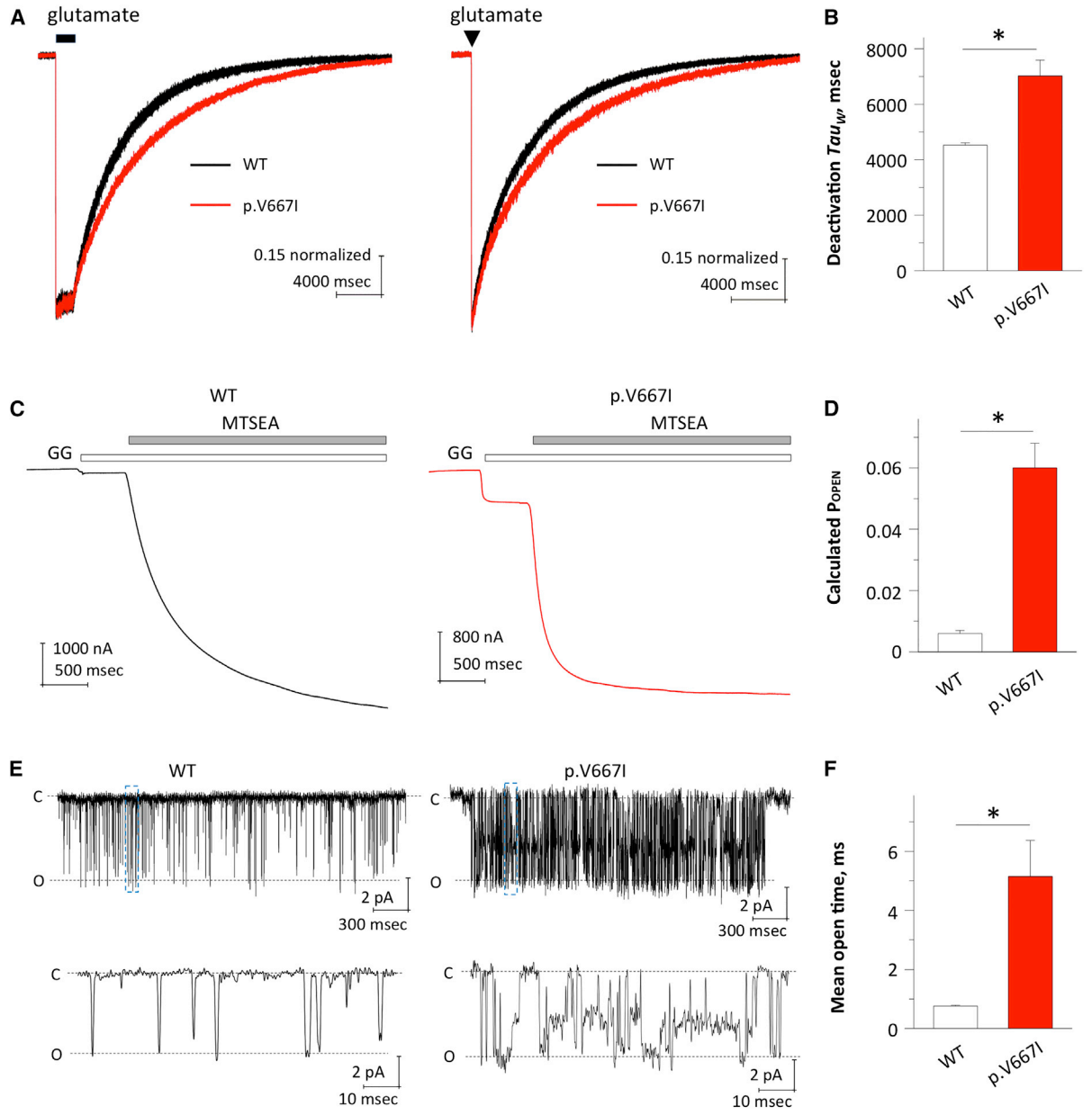

Figure 3. The Mutant GluN2D-p.Val667Ile Changes Response Time Course and Channel Open Probability
(A) The p.Val667Ile mutation prolongs deactivation time course of GluN2D receptors. Normalized representative current response of di-heteromeric NMDARs (WT GluN2D and GluN2D-p.Val667Ile) to 1 mM glutamate applied for 1.5 s (left) or 5 ms (right) (V_{HOLD} −60 mV); 50 μM glycine was present in all solutions.
(B) Summary of weighted deactivation tau of WT GluN2D and mutant receptors. Error bars show SEM, which were calculated from six independent recordings.
(C) Representative current traces evoked by agonists (100 μM glutamate and glycine) followed by 200 μM MTSEA were determined by TEVC recordings from *Xenopus* oocytes expressing GluN1-p.Ala652Cys/GluN2D (left) and GluN1-p.Ala652Cys/GluN2D-p.Val667Ile receptors (right).
(D) Summary of estimated P_{OPEN} of WT GluN2D and mutant receptors determined in oocytes. Error bars show SEM, which were calculated from 22 and 32 independent recordings of WT and mutant receptors, respectively.
(E) Representative current traces of steady-state recordings from an outside-out patch containing WT (left) and the mutant (right) NMDARs. Unitary currents were activated by 1 mM glutamate and 50 μM glycine. Abbreviations are as follows: C, close; O, open.
(F) Summary of channel mean open time of WT GluN2D and mutant receptors. *$p < 0.05$ compared to WT GluN2D, unpaired t test. Error bars show SEM, which were calculated from three and four independent recordings for WT and mutant receptors, respectively.

pre-treatment details) was started on memantine at age 6.5 years and titrated up in dose (started at 2 mg daily for 1 week and increased by 2 mg weekly to a goal of 20 mg daily, equivalent to 0.85 mg/kg/day). Prior to initiation of memantine treatment, she had intermittent events of lethargy, emesis, and right-sided weakness that

Table 2. Summary of FDA-Approved NMDA Receptor Channel Blocker Analyses

Name	Class	WT IC_{50}	p.Val667Ile IC_{50}
Memantine	AD drug	0.57 ± 0.04 (10; 92%)	4.0 ± 0.9* (9; 92%)
Dextromethorphan	antitussive	4.0 ± 0.4 (12; 90%)	13 ± 1.6* (7; 88%)
Dextrorphan	metabolite	0.60 ± 0.09 (10; 94%)	2.5 ± 0.4* (8; 93%)
Amantadine	antiviral	34 ± 1.8 (8; 88%)	189 ± 26* (8; 86%)
Ketamine	anesthetic	2.2 ± 0.31 (11; 91%)	8.1 ± 2.3* (11; 89%)
Mg^{2+}[a]		221 ± 20 (12; 84%)	346 ± 39* (15; 78%)

IC_{50}, mean ± SEM, μM (n; max inhibition% at 100 μM for memantine, 300 μM for dextromenthorphan, 30 μM for dextrorphan, 1,000 μM for amantadine, 100 μM for ketamine, 1,000 μM for Mg^{2+}). Abbreviation is as follows: AD, Alzheimer disease. *$p < 0.05$, compared to WT, unpaired t test.
[a]Holding potential was at −40 mV, except for Mg^{2+} (−60 mV).

were concerning for postictal effects of subclinical seizures but were not captured on pretreatment video EEG (Figures 6A, 6A′, and 6A″). Repeat video EEG recording after 2 months of memantine treatment revealed an unchanged background at times when awake but at other times the EEG was higher voltage and contained frequent bifrontal and multifocal discharges with no organization (Figure 6B). When asleep, the EEG became hypsarrhythmic (Figure 6B′). No clinical seizures were recorded but four subclinical seizures occurred that began at the T6 electrode (not shown). With worsening seizures and EEG findings, the memantine was weaned off. Shortly after the memantine wean, her clinical complex partial seizures became more frequent and were associated with prolonged postictal weakness. Therefore, memantine was reintroduced and dose was escalated to 20 mg twice daily (equivalent to 1.3 mg/kg/day) while the ketogenetic diet was also initated. Both treatments were well tolerated but neither resulted in clinically meaningful improvement. Over the next 18 months, her seizures and resulting encephalopathy increased in frequency, duration, and severity, with multiple admissions for subclinical status that did not resolve with traditional anti-seizure medications. At 8.5 years, in the setting of an increasing severity and frequency of clinical complex partial seizures as well as worsening encephalopathy and functional decline (Figure 6C), the decision was made to induce pharmacological coma in an attempt to maximize therapy to treat her electrographic status epilepticus. Escalating doses of midazolam and pentobarbital infusions put her into burst suppression (Figure 6C″) but did not significantly alter her EEG (Figure 6C′) or clinical picture upon weaning. Given her pre-admission clinical state and the failure of phentobarbital and midazolam infusions, a ketamine infusion was attempted based on the knowledge of the *GRIN2D* status. Ketamine infusion at 10 mg/kg/hr aborted her electrographic status epilepticus, but frequent subclinical seizures and a highly epileptiform background remained (Figure 6D). With the proband remaining in extremis and the in vitro data on the c.1999G>A (p.Val667Ile) variant described above, she was started on an intravenous magnesium sulfate infusion (2 g per dose given every 4 hr). Immediately after onset of Mg^{2+} infusion, her EEG improved dramatically (Figure 6D′). Subclinical seizures remained on this more normal-appearing background, but were reduced to few brief seizures per hour. Based on the dramatic change in her EEG with Mg^{2+} infusion, ketamine was weaned off. After a few days, her EEG remained significantly improved (not shown) and she started to show clinical improvement but continued to have a few subclinical seizures per day, which worsened when serum Mg^{2+} levels dropped below 2 mg/dL. Restarting a lower dose of ketamine (2 mg/kg/hr) in combination with the magnesium infusion led to resolution of subclinical seizures for days and an EEG that had some background slowing but was remarkably non-epileptiform (see Figure 6D″). Because this treatment was given in the intensive care unit setting, the proband was subsequently transitioned to an enteral regimen of ketamine (1 mg/kg/dose given every 6 hr) and magnesium as amino acids chelate (1.5 mEq/kg/dose given every 6 hr). Weeks after transitioning to oral ketamine and Mg^{2+}, she remains clinically seizure free and she is making progress in an inpatient rehabilation setting, standing in a gait trainer, reaching for toys, and cognitively back to her pre-coma baseline (Figure 6E).

Proband 2 was also started on memantine after the diagnosis of a *GRIN2D* mutation was made at 2.5 years old. She was started at 0.5 mg/kg/day of memantine during a hospitalization to ensure safety. Pre-treament records reported 29 seizures during the 5 days prior to initiation of memantine treatment (5.8 seizures per day). This frequency decreased to 12 seizures during the 5 days before being discharged from hospital (~59% seizure reduction). In the following 3 weeks, she had complete seizure freedom and developmental improvement including improved visual fixation, motor development progress including initiation of independent sitting, as well as improved turning around and grasping. However, 4 weeks after discharge, she developed a viral infection and her seizures recurred (4–8 seizures daily) and were characterized by jerking lasting for 5–6 s, a "vibrating" face, strabismus, and slowed breathing. Months later, when compared to her pre-memantine clinical status while also on sultiam (10 mg/kg/day) and lamotrigine (3.4 mg/kg/day), her seizure frequency has settled at one seizure every 2–3 days (characterized by startle, screaming, opening of eyes, tonic movements of lower extremities, and deviation of eyes and head to the left lasting approximately 1 min). In addition, her EEG at last visit was mostly normal with some spike discharges still occurring at night. Whereas she had severe autistic behavior pretreatment, she is now markedly more awake, alert, and focused.

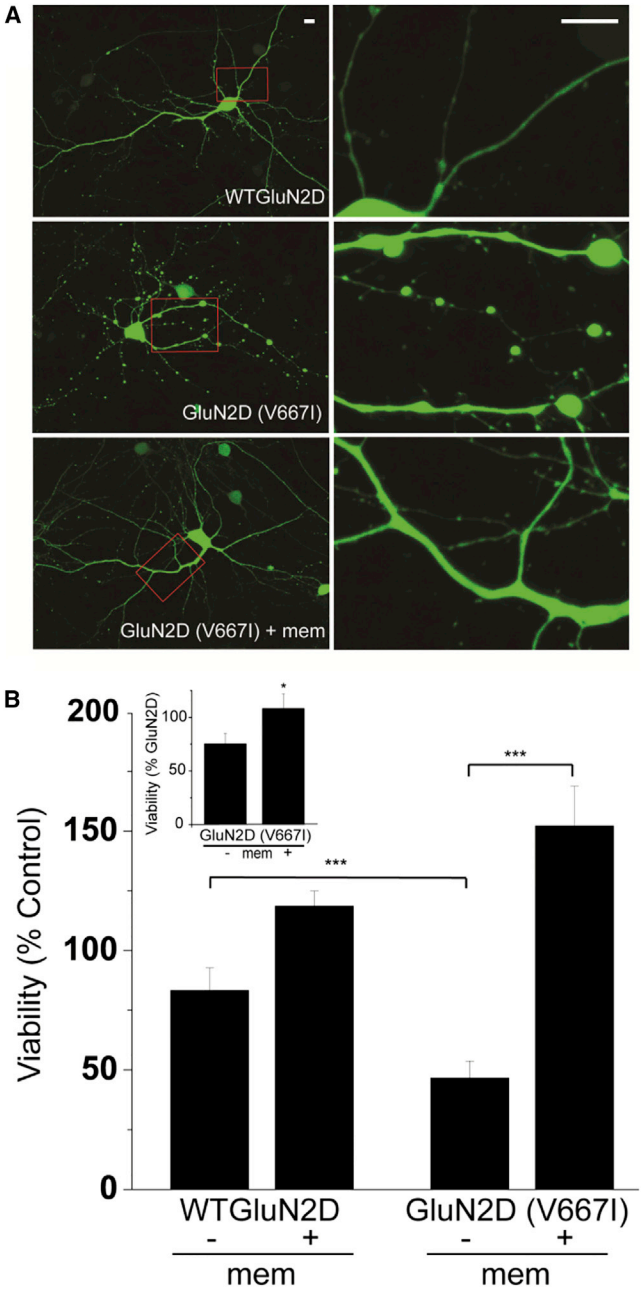

Figure 4. Transfection of GluN2D-p.Val667Ile into Cultured Cortical Neurons Induces Excitotoxicity, which Can Be Prevented by Memantine

(A) Confocal images display morphological features of rat cortical neurons transfected with a GFP-expressing plasmid (1.5/2.5 μg/mL of total transfected DNA), along with either WT GluN2D or GluN2D-p.Val667Ile (1/2.5 μg/mL of total transfected DNA); the latter was supplemented with either vehicle or memantine (50 μM). Note the prominent dendritic swelling induced by expression of GluN2D-p.Val667Ile, but not by WT GluN2D, which was mitigated by memantine treatment. Left column images were acquired 24 hr after transfection at 20× total magnification; areas boxed in red are magnified to 100 × in the adjacent panels. Scale bars represent 10 μM.

(B) Histograms representing mean cell viability values as a percent of control groups. Main graph: neuronal cultures were transfected with luciferase cDNA (0.625/2.5 μg/mL of total transfected DNA) to assay cell viability, along with either PCIneo-vector, WT GluN2D, or GluN2D-p.Val667Ile cDNA (1/2.5 μg/mL of total transfected DNA). Each transfection condition was performed in the presence or either vehicle (–) or memantine (50 μM; +). Luciferase assays were performed 48 hr after transfection. Each experiment was carried out in quadruplicate, and five independent experiments were performed. Each condition was normalized to its corresponding vector-transfected group to obtain relative viability values (e.g., memantine-treated, vector-expressing group was used to normalize memantine-treated GluN2D-expressing group). Histograms are displayed as mean ± SEM of viability (percent control) values for each condition: WT GluN2D (–), 83.3 ± 9.5; WT GluN2D (+), 118.6 ± 6.3; GluN2D-p.Val667Ile (–), 46.7 ± 7.0; GluN2D-p.Val667Ile (+), 152.2 ± 16.6; **$p < 0.01$, ***$p < 0.001$; ANOVA/Bonferroni. Inset: cell viability assays were confirmed by cell counting. Neuronal cultures were transfected with a GFP-expressing plasmid (1.5/2.5 μg/mL of total transfected DNA), along with either WT GluN2D or GluN2D-p.Val667Ile cDNA (1/2.5 μg/mL of total transfected DNA). Each transfection condition was performed in the presence or either vehicle (–) or memantine (50 μM; +). Cells were fixed with 4% paraformaldehyde 72 hr after transfection and counted by a person blinded to the experimental groups. 30 image fields from 3 coverslips per condition were obtained at 20× magnification in four independent experiments. The number of neurons per coverslip was averaged for each condition. GluN2D-p.Val667Ile groups (with and without memantine) were standardized to WT GluN2D-transfected control to obtain relative viability values expressed as percent control for each experiment. Data are displayed as mean ± SEM of viability (percent control) for each condition: GluN2D-p.Val667Ile (–), 75.3 ± 9.6; GluN2D-p.Val667Ile (+), 108.1 ± 13.7; *$p < 0.05$; paired t test.

Discussion

We report a de novo, recurrent, missense mutation—c.1999G>A (p.Val667Ile)—in *GRIN2D* that was identified independently in two unrelated probands with epileptic encephalopathy and found to significantly alter the NMDA receptor currents and responsiveness to antagonists, although mutations in other NMDA receptor subunits have recently been recognized to play an important role in the etiology of childhood epilepsy syndromes such as West syndrome (MIM: 308350) and Landau Kleffner syndrome (MIM: 245570).[5,7–10,36–38] The c.1999G>A (p.Val667Ile) mutation that we propose is the etiology of the severe neurological impairment in these two unrelated individuals is located in the M3 transmembrane domain motif, which participates in channel gating.[6] Indeed, our functional data both validate the pathogenicity of this mutation and demonstrate that this mutation significantly increases NMDAR function. This mutation increased both glutamate and glycine potency, reduced the sensitivity of the channel to negative allosteric modulators, prolonged the response time course to synaptic-like stimulation, and increased the probability that an agonist-bound single channel will open by 6-fold. Thus, functional in vitro studies confirm that the c.1999G>A (p.Val667Ile) mutation results in a strong gain-of-function of recombinant GluN1/GluN2D NMDARs. Furthermore, there are marked clinical parallels to previously described disorders caused by other glutamate ionotropic receptor NMDA type subunits. For example, encephalopathies caused by *GRIN1*, *GRIN2A*, and *GRIN2B* mutations are associated with a similarly severe developmental delay, severe

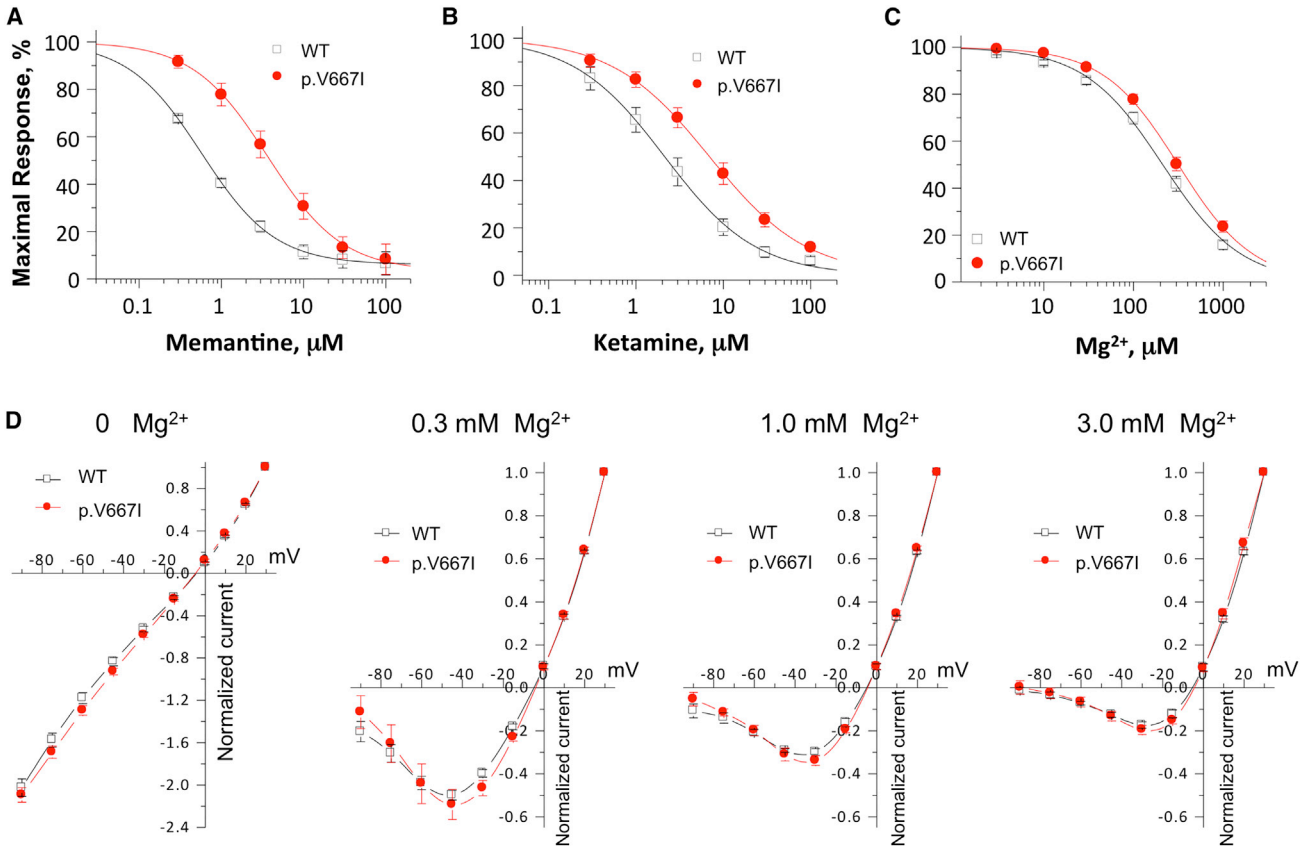

Figure 5. Screening of FDA-Approved NMDAR Antagonists
(A–C) Composite concentration-response curves for memantine (A), ketamine (B), and Mg^{2+} (C) inhibition on the mutant and WT current responses to maximal effective concentration (100 μM) of glutamate and glycine determined by TEVC recordings from oocytes. (D) Current-voltage (I-V) curves in the presence of 0, 0.3 mM, 1.0 mM, and 3.0 mM of Mg^{2+}.

intellectual disability, marked truncal hypotonia, movement disorder, seizures, and non-specific volume loss on MRI. The involuntary eye movements reported early in life in proband 1 resemble oculogyric crises seen in *GRIN1* encephalopathy.[38] The hypsarrhythmic EEG pattern and infantile spasms have previously been described in *GRIN2B* encephalopathy (MIM: 616139),[37] and the worsening of the EEG in sleep is a frequent observation in epilepsies (MIM: 245570) due to *GRIN2A* mutations.[10]

Because conventional antiepileptic medications failed to optimally control either of the *GRIN2D* individuals' seizures, the in vitro sensitivity of the mutant receptors was evaluated to candidate FDA-approved NMDAR antagonists, including memantine, ketamine, dextromethorphan, and amantadine. This functional analysis showed that these mutant NMDARs are less sensitive to channel blockers, but still can be inhibited, raising the possibility of using memantine to partially rectify the overactivation of the NMDAR produced by this mutation. The clinical responses of these two individuals to memantine raises interesting questions about the potential responsiveness and the ideal time and duration for treatment. Whereas both individuals reported subjective developmental gains, the seizure responses were different. This difference, may, in part, be due to the timing of treatment (proband 2 was treated at a younger age than proband 1) or just to the natural history of the disease (proband 1 had good initial developmental and seizure response on levateracitam but deteriorated over time as her epilepsy control worsened). Proband 1's apparent response to a combined magnesium and ketamine regimen, devised based on the in vitro functional validation data in *Xenopus laevis* oocytes, highlights the importance of understanding the biology and physiology of any given mutation, as this can lead to successful precision treatments as was observed in this case. Specifically, the in vitro results showed a 10-fold diminished potency of memantine, although the mutant receptors still retain some sensitivity (IC_{50} 4 μM). The mutant receptors had less pronounced effects on the potency of ketamine, reducing potency about 3.5-fold. Given the low cerebrospinal fluid (CSF) levels of memantine, we postulate that the reduced potency seen in the *GRIN2D* subjects may lead to an inability to occupy the receptor at a level that could produce effects to alter circuit function and clinical outcome. However, ketamine reaches higher CSF levels, and its potency is impacted to a lesser extent than is the potency of memantine by the mutation, as appears to be consistent with the effectiveness of ketamine treatment in conjunction with Mg^{2+} administration in proband 1.

Recently, a number of groups have reported the utility of applying a "precision" medicine approach to individuals

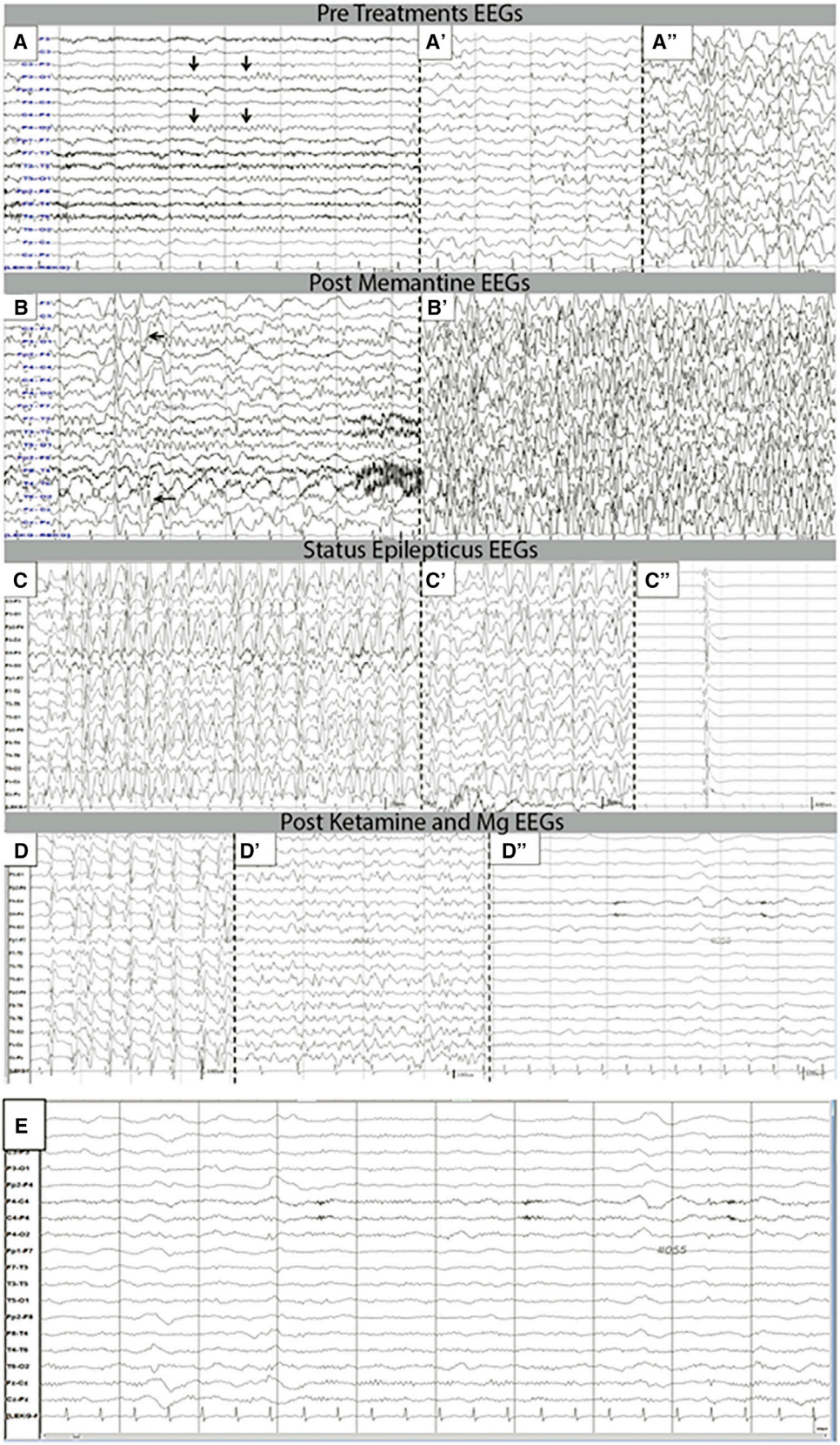

Figure 6. EEG before and after Treatments Are Presented
(A) The top row is the pre-treatment EEG (baseline at 6 years old). The best awake background is shown (A) with a 7–8 Hz posterior theta-alpha rhythm present for intermittent periods. When she went to sleep (A′, A″), there was an absence of normal sleep architecture (A′) and at time the recording became hypsarrythmic with high amplitude, multifocal sharps, and a lack of organization (A″).

(legend continued on next page)

with epileptic encephalopathies, where identification of a pathogenic variant in an ion channel directed clinicians to an existing pharmacologic agent that counter-balanced the in vivo effect of the mutation. The first such paper involved treatment of a single case subject who has an NMDA receptor mutation affecting the GluN2A subunit, which resulted in significant seizure improvement on memantine.[36] Subsequently, retagabine use has been reported in *KCNQ2*-related epileptic encephalopathy with mixed results.[39,40] Finally, infants with *KCNT1*-related epileptic encephalopathy or malignant migrating partial seizures of infancy have been treated with quinidine to increase current through the channel.[41–43] There has been both good responses[41] and a lack of response seen with quinidine,[42,43] raising the question as to whether the response could be mutation specific or impacted by age or treatment timing. Our current study further supports the concept of recycling existing medications to target specific mutations in ion channels. Our treatment efforts had positive but not definitive responses, similarly as seen in the other mutation-guided treatment reports in epilepsy, again emphasizing the need to address the relative effects of treatment timing, duration, and mutation-specific issues in other individuals found to have *GRIN2D* gain-of-function mutations. Collectively, these studies highlight the inherent limitations of open label, small case series. Well-designed clinical trials are needed before the field can definitively conclude whether we have truly achieved an era of precision medicine for the diverse group of epileptic encephalopathies.

Overall, this work demonstrates the importance of focusing therapeutic efforts on treatments that modulate functional effects of a precisely established genetic etiology, rather than non-specific treatments largely focused on alleviation of generic clinical manifestations. The combination of state-of-the-art genomic sequencing with functional validation of specific disease mechanism and evaluation of candidate therapeutic approaches in vitro may enable the realization of precision medicine for otherwise intractable or progressive pediatric neurodevelopmental disease.

Accession Numbers

The LOVD accession number for the *GRIN2D* sequence reported in this paper is #0000119835.

Supplemental Data

Supplemental Data include additional case descriptions, one figure, and two tables and can be found with this article online at http://dx.doi.org/10.1016/j.ajhg.2016.07.013.

Conflicts of Interest

S.F.T. is a co-founder and paid consultant of NeurOp, Inc. S.F.T. is a paid consultant for and received research support from Janssen Pharmaceuticals. S.F.T. is a paid consultant of Pfizer, Inc. K.H. is an employee of CeGaT.

Acknowledgments

We thank both families involved in this study for their participation. We acknowledge Frank D. Mentch, Fengxiang Wang, and James Snyder, who helped in the DNA sample extraction and handling; and Cuiping Hou, Tiancheng Wang, Jing Zhang, John DiRaddo, and Phuong Le, who provided technical assistance. Research reported in this publication was supported by the Eunice Kennedy Shriver National Institute of Child Health & Human Development of the NIH (R01HD082373 to H.Y.), the National Center for Advancing Translational Sciences of the NIH (UL1TR000454 to H.Y.), the National Institute of Neurological Disorders and Stroke (NS043277 to E.A., NS036654 to S.F.T., NS007413 and NS049453 to X.R.O.-G.), the Xiangya-Emory Medical Schools Visiting Student Program (to W.C.), and Institutional Development Funds to the Center for Applied Genomics (CAG grant #7225940617 and eMERGE grant [U01-HG006830 to H.H.]) at the Children's Hospital of Philadelphia (CHOP). The content is solely the responsibility of the authors and does not necessarily represent the official views of the funding agencies.

Received: April 30, 2016
Accepted: July 11, 2016
Published: September 8, 2016

Web Resources

1000 Genomes, http://www.1000genomes.org
ExAC Browser, http://exac.broadinstitute.org/
GenBank, http://www.ncbi.nlm.nih.gov/genbank/
LOVD, http://grenada.lumc.nl/LSDB_list/lsdbs/GRIN2D
Modeller, https://salilab.org/modeller/
MUSCLE, http://www.ebi.ac.uk/Tools/msa/muscle/
NHLBI Exome Sequencing Project (ESP) Exome Variant Server, http://evs.gs.washington.edu/EVS/
OMIM, http://www.omim.org/

(B) The second row presents the post memantine treatment EEG, 3 months after starting treatment, on a stable dose for 6 weeks. Again, the best awake background (B) is presented, but this had fewer periods with a posterior theta alpha rhythm and more frequent interruption by bifrontal or lateralized (arrows in B) epileptiform sharps. After treatment, when asleep, the EEG was continuously high voltage, multifocal sharps, and lacked any discernable organization (B′).
(C) The third row presents the EEG after being off memantine and admitted for status epilepticus. The EEG shows continuous generalized spike and slow wave discharges at ~3 Hz. After failing first and second line i.v. medications, she was placed on a continuous midazolam infusion (C′) with slowing of the spike and wave but status persisted. Changing to pentobarbital resulted in burst suppression, but when pentobarbital was weaned, the continous spike and slow wave returned. She was put under pentobarbital and ketamine and burst suppression returned (C″).
(D) Wean of pentobarbital again resulted in return of spike wave. Addition of i.v. magnesium to ketamine resulted in acute sessation of spike wave without EEG suppression (D′). Finally, lowering the IV Mg^{2+} and ketamine resulted in persistence of a slow and better organized EEG (D″). This EEG background continued when Mg^{2+} and ketamine were changed to oral administration (not shown).
(E) Weeks after transitioning to oral ketamine and Mg^{2+}, she remains clinically seizure free.

References

1. Srivastava, S., Cohen, J.S., Vernon, H., Barañano, K., McClellan, R., Jamal, L., Naidu, S., and Fatemi, A. (2014). Clinical whole exome sequencing in child neurology practice. Ann. Neurol. *76*, 473–483.
2. Yang, Y., Muzny, D.M., Reid, J.G., Bainbridge, M.N., Willis, A., Ward, P.A., Braxton, A., Beuten, J., Xia, F., Niu, Z., et al. (2013). Clinical whole-exome sequencing for the diagnosis of mendelian disorders. N. Engl. J. Med. *369*, 1502–1511.
3. Lee, H., Deignan, J.L., Dorrani, N., Strom, S.P., Kantarci, S., Quintero-Rivera, F., Das, K., Toy, T., Harry, B., Yourshaw, M., et al. (2014). Clinical exome sequencing for genetic identification of rare Mendelian disorders. JAMA *312*, 1880–1887.
4. Yang, Y., Muzny, D.M., Xia, F., Niu, Z., Person, R., Ding, Y., Ward, P., Braxton, A., Wang, M., Buhay, C., et al. (2014). Molecular findings among patients referred for clinical whole-exome sequencing. JAMA *312*, 1870–1879.
5. Allen, A.S., Berkovic, S.F., Cossette, P., Delanty, N., Dlugos, D., Eichler, E.E., Epstein, M.P., Glauser, T., Goldstein, D.B., Han, Y., et al.; Epi4K Consortium; Epilepsy Phenome/Genome Project (2013). De novo mutations in epileptic encephalopathies. Nature *501*, 217–221.
6. Traynelis, S.F., Wollmuth, L.P., McBain, C.J., Menniti, F.S., Vance, K.M., Ogden, K.K., Hansen, K.B., Yuan, H., Myers, S.J., and Dingledine, R. (2010). Glutamate receptor ion channels: structure, regulation, and function. Pharmacol. Rev. *62*, 405–496.
7. Yuan, H., Low, C.M., Moody, O.A., Jenkins, A., and Traynelis, S.F. (2015). Ionotropic GABA and glutamate receptor mutations and human neurologic diseases. Mol. Pharmacol. *88*, 203–217.
8. Carvill, G.L., Regan, B.M., Yendle, S.C., O'Roak, B.J., Lozovaya, N., Bruneau, N., Burnashev, N., Khan, A., Cook, J., Geraghty, E., et al. (2013). GRIN2A mutations cause epilepsy-aphasia spectrum disorders. Nat. Genet. *45*, 1073–1076.
9. Lemke, J.R., Lal, D., Reinthaler, E.M., Steiner, I., Nothnagel, M., Alber, M., Geider, K., Laube, B., Schwake, M., Finsterwalder, K., et al. (2013). Mutations in GRIN2A cause idiopathic focal epilepsy with rolandic spikes. Nat. Genet. *45*, 1067–1072.
10. Lesca, G., Rudolf, G., Bruneau, N., Lozovaya, N., Labalme, A., Boutry-Kryza, N., Salmi, M., Tsintsadze, T., Addis, L., Motte, J., et al. (2013). GRIN2A mutations in acquired epileptic aphasia and related childhood focal epilepsies and encephalopathies with speech and language dysfunction. Nat. Genet. *45*, 1061–1066.
11. Endele, S., Rosenberger, G., Geider, K., Popp, B., Tamer, C., Stefanova, I., Milh, M., Kortüm, F., Fritsch, A., Pientka, F.K., et al. (2010). Mutations in GRIN2A and GRIN2B encoding regulatory subunits of NMDA receptors cause variable neurodevelopmental phenotypes. Nat. Genet. *42*, 1021–1026.
12. Li, H., and Durbin, R. (2009). Fast and accurate short read alignment with Burrows-Wheeler transform. Bioinformatics *25*, 1754–1760.
13. DePristo, M.A., Banks, E., Poplin, R., Garimella, K.V., Maguire, J.R., Hartl, C., Philippakis, A.A., del Angel, G., Rivas, M.A., Hanna, M., et al. (2011). A framework for variation discovery and genotyping using next-generation DNA sequencing data. Nat. Genet. *43*, 491–498.
14. Wang, K., Li, M., and Hakonarson, H. (2010). ANNOVAR: functional annotation of genetic variants from high-throughput sequencing data. Nucleic Acids Res. *38*, e164.
15. Cingolani, P., Platts, A., Wang, L., Coon, M., Nguyen, T., Wang, L., Land, S.J., Lu, X., and Ruden, D.M. (2012). A program for annotating and predicting the effects of single nucleotide polymorphisms, SnpEff: SNPs in the genome of *Drosophila melanogaster* strain w1118; iso-2; iso-3. Fly (Austin) *6*, 80–92.
16. Lemke, J.R., Riesch, E., Scheurenbrand, T., Schubach, M., Wilhelm, C., Steiner, I., Hansen, J., Courage, C., Gallati, S., Bürki, S., et al. (2012). Targeted next generation sequencing as a diagnostic tool in epileptic disorders. Epilepsia *53*, 1387–1398.
17. Hedegaard, M., Hansen, K.B., Andersen, K.T., Bräuner-Osborne, H., and Traynelis, S.F. (2012). Molecular pharmacology of human NMDA receptors. Neurochem. Int. *61*, 601–609.
18. Hansen, K.B., Tajima, N., Risgaard, R., Perszyk, R.E., Jørgensen, L., Vance, K.M., Ogden, K.K., Clausen, R.P., Furukawa, H., and Traynelis, S.F. (2013). Structural determinants of agonist efficacy at the glutamate binding site of N-methyl-D-aspartate receptors. Mol. Pharmacol. *84*, 114–127.
19. Yuan, H., Hansen, K.B., Vance, K.M., Ogden, K.K., and Traynelis, S.F. (2009). Control of NMDA receptor function by the NR2 subunit amino-terminal domain. J. Neurosci. *29*, 12045–12058.
20. Yuan, H., Erreger, K., Dravid, S.M., and Traynelis, S.F. (2005). Conserved structural and functional control of N-methyl-D-aspartate receptor gating by transmembrane domain M3. J. Biol. Chem. *280*, 29708–29716.
21. Aras, M.A., Saadi, R.A., and Aizenman, E. (2009). Zn2+ regulates Kv2.1 voltage-dependent gating and localization following ischemia. Eur. J. Neurosci. *30*, 2250–2257.
22. Aras, M.A., Hara, H., Hartnett, K.A., Kandler, K., and Aizenman, E. (2009). Protein kinase C regulation of neuronal zinc signaling mediates survival during preconditioning. J. Neurochem. *110*, 106–117.
23. Aras, M.A., Hartnett, K.A., and Aizenman, E. (2008). Assessment of cell viability in primary neuronal cultures. Curr. Protoc. Neurosci. *Chapter 7*, 18.
24. Li, F., and Tsien, J.Z. (2009). Memory and the NMDA receptors. N. Engl. J. Med. *361*, 302–303.
25. Cull-Candy, S., Brickley, S., and Farrant, M. (2001). NMDA receptor subunits: diversity, development and disease. Curr. Opin. Neurobiol. *11*, 327–335.
26. Li, D., Opas, E.E., Tuluc, F., Metzger, D.L., Hou, C., Hakonarson, H., and Levine, M.A. (2014). Autosomal dominant hypoparathyroidism caused by germline mutation in GNA11: phenotypic and molecular characterization. J. Clin. Endocrinol. Metab. *99*, E1774–E1783.
27. Bhoj, E.J., Li, D., Harr, M.H., Tian, L., Wang, T., Zhao, Y., Qiu, H., Kim, C., Hoffman, J.D., Hakonarson, H., and Zackai, E.H. (2015). Expanding the SPECC1L mutation phenotypic spectrum to include Teebi hypertelorism syndrome. Am. J. Med. Genet. A. *167A*, 2497–2502.
28. Jones, K.S., VanDongen, H.M., and VanDongen, A.M. (2002). The NMDA receptor M3 segment is a conserved transduction element coupling ligand binding to channel opening. J. Neurosci. *22*, 2044–2053.
29. Karakas, E., and Furukawa, H. (2014). Crystal structure of a heterotetrameric NMDA receptor ion channel. Science *344*, 992–997.
30. Vance, K.M., Simorowski, N., Traynelis, S.F., and Furukawa, H. (2011). Ligand-specific deactivation time course of GluN1/GluN2D NMDA receptors. Nat. Commun. *2*, 294.
31. Choi, D.W. (1994). Glutamate receptors and the induction of excitotoxic neuronal death. Prog. Brain Res. *100*, 47–51.

32. Ghasemi, M., and Schachter, S.C. (2011). The NMDA receptor complex as a therapeutic target in epilepsy: a review. Epilepsy Behav. *22*, 617–640.
33. Chez, M.G., Burton, Q., Dowling, T., Chang, M., Khanna, P., and Kramer, C. (2007). Memantine as adjunctive therapy in children diagnosed with autistic spectrum disorders: an observation of initial clinical response and maintenance tolerability. J. Child Neurol. *22*, 574–579.
34. Erickson, C.A., Posey, D.J., Stigler, K.A., Mullett, J., Katschke, A.R., and McDougle, C.J. (2007). A retrospective study of memantine in children and adolescents with pervasive developmental disorders. Psychopharmacology (Berl.) *191*, 141–147.
35. Yuan, H., Hansen, K.B., Zhang, J., Pierson, T.M., Markello, T.C., Fajardo, K.V., Holloman, C.M., Golas, G., Adams, D.R., Boerkoel, C.F., et al. (2014). Functional analysis of a de novo GRIN2A missense mutation associated with early-onset epileptic encephalopathy. Nat. Commun. *5*, 3251.
36. Pierson, T.M., Yuan, H., Marsh, E.D., Fuentes-Fajardo, K., Adams, D.R., Markello, T., Golas, G., Simeonov, D.R., Holloman, C., Tankovic, A., et al.; PhD for the NISC Comparative Sequencing Program (2014). GRIN2A mutation and early-onset epileptic encephalopathy: personalized therapy with memantine. Ann. Clin. Transl. Neurol. *1*, 190–198.
37. Lemke, J.R., Hendrickx, R., Geider, K., Laube, B., Schwake, M., Harvey, R.J., James, V.M., Pepler, A., Steiner, I., Hörtnagel, K., et al. (2014). GRIN2B mutations in West syndrome and intellectual disability with focal epilepsy. Ann. Neurol. *75*, 147–154.
38. Ohba, C., Shiina, M., Tohyama, J., Haginoya, K., Lerman-Sagie, T., Okamoto, N., Blumkin, L., Lev, D., Mukaida, S., Nozaki, F., et al. (2015). GRIN1 mutations cause encephalopathy with infantile-onset epilepsy, and hyperkinetic and stereotyped movement disorders. Epilepsia *56*, 841–848.
39. Weckhuysen, S., Ivanovic, V., Hendrickx, R., Van Coster, R., Hjalgrim, H., Møller, R.S., Grønborg, S., Schoonjans, A.S., Ceulemans, B., Heavin, S.B., et al.; KCNQ2 Study Group (2013). Extending the KCNQ2 encephalopathy spectrum: clinical and neuroimaging findings in 17 patients. Neurology *81*, 1697–1703.
40. Numis, A.L., Angriman, M., Sullivan, J.E., Lewis, A.J., Striano, P., Nabbout, R., and Cilio, M.R. (2014). KCNQ2 encephalopathy: delineation of the electroclinical phenotype and treatment response. Neurology *82*, 368–370.
41. Bearden, D., Strong, A., Ehnot, J., DiGiovine, M., Dlugos, D., and Goldberg, E.M. (2014). Targeted treatment of migrating partial seizures of infancy with quinidine. Ann. Neurol. *76*, 457–461.
42. Mikati, M.A., Jiang, Y.H., Carboni, M., Shashi, V., Petrovski, S., Spillmann, R., Milligan, C.J., Li, M., Grefe, A., McConkie, A., et al. (2015). Quinidine in the treatment of KCNT1-positive epilepsies. Ann. Neurol. *78*, 995–999.
43. Chong, P.F., Nakamura, R., Saitsu, H., Matsumoto, N., and Kira, R. (2016). Ineffective quinidine therapy in early onset epileptic encephalopathy with KCNT1 mutation. Ann. Neurol. *79*, 502–503.
44. Lee, C.H., Lü, W., Michel, J.C., Goehring, A., Du, J., Song, X., and Gouaux, E. (2014). NMDA receptor structures reveal subunit arrangement and pore architecture. Nature *511*, 191–197.